Knockdown of desmin in zebrafish larvae affects interfilament spacing and mechanical properties of skeletal muscle

Mei Li,[1] Monika Andersson-Lendahl,[2] Thomas Sejersen,[3] and Anders Arner[1]

[1]Department of Physiology and Pharmacology, [2]Department of Cell and Molecular Biology, and [3]Department of Women's and Children's Health, Karolinska Institutet, SE 171 77 Stockholm, Sweden

Skeletal muscle was examined in zebrafish larvae in order to address questions related to the function of the intermediate filament protein desmin and its role in the pathogenesis of human desminopathy. A novel approach including mechanical and structural studies of 4–6-d-old larvae was applied. Morpholino antisense oligonucleotides were used to knock down desmin. Expression was assessed using messenger RNA and protein analyses. Histology and synchrotron light–based small angle x-ray diffraction were applied. Functional properties were analyzed with in vivo studies of swimming behavior and with in vitro mechanical examinations of muscle. The two desmin genes normally expressed in zebrafish could be knocked down by ∼50%. This resulted in a phenotype with disorganized muscles with altered attachments to the myosepta. The knockdown larvae were smaller and had diminished swimming activity. Active tension was lowered and muscles were less vulnerable to acute stretch-induced injury. X-ray diffraction revealed wider interfilament spacing. In conclusion, desmin intermediate filaments are required for normal active force generation and affect vulnerability during eccentric work. This is related to the role of desmin in anchoring sarcomeres for optimal force transmission. The results also show that a partial lack of desmin, without protein aggregates, is sufficient to cause muscle pathology resembling that in human desminopathy.

The Journal of General Physiology

INTRODUCTION

Myofibrillar myopathies constitute a heterogeneous group of comparatively rare muscle diseases, usually with a late onset and often with severe clinical manifestations, initially from distal muscles and the heart. A common morphological feature is the appearance of structural changes in the myofibrillar organization, usually combined with aberrant cellular aggregates of different proteins, often including desmin (Schröder and Schoser, 2009; Selcen, 2011). These myopathies are usually dominantly inherited with mutations identified in different sarcomere-associated proteins, including desmin, αβ-crystallin, plectin, filamin C, ZASP, FHL1, BAG3, and myotilin (Schröder and Schoser, 2009). Many of these proteins have been proposed to contribute to anchoring of sarcomeres and of other cellular components, e.g., nuclei and mitochondria. The protein deposits, considered to be formed by aggregation of mutated proteins, possibly altered by posttranslational modification, are key morphological characteristics (Ferrer and Olivé, 2008). However, the role of these aggregates in the pathogenesis of the disease is unknown and the lack of functional proteins, caused by trapping or dysfunctional mutated proteins, can also be an important pathological feature contributing to contractile failure. It is currently unknown to what extent these two pathological alterations participate in the morphological and functional pathology of myofibrillar myopathies.

Desminopathies, which cause an abnormal accumulation of desmin in the muscle fibers, constitute a major group of the myofibrillar myopathies (Paulin et al., 2004; van Spaendonck-Zwarts et al., 2011). In striated muscle cells, desmin intermediate filaments form a scaffold around the Z-disk, connecting the contractile apparatus to the cytoskeleton and costameres, thus playing an important role in maintaining myofibrillar integrity and in transmitting forces in the muscle (Lazarides, 1980). In addition, the intermediate filaments connect to mitochondria, nuclei, and other cellular components (Tokuyasu et al., 1983). Most of the desminopathies are caused by dominantly negative mutations (Sjöberg et al., 1999; Dalakas et al., 2000), although a case with homozygous or hemizygous desmin mutations, lacking wild-type desmin, has also been reported (Muñoz-Mármol et al., 1998). Increased cardiac expression of wild-type desmin in a mouse model did not cause pathological changes, which suggests that increased desmin contents are not, per se, detrimental. However, overexpression of a mutated desmin (7–amino acid deletion: R173 through E179) interfered with the intermediate filament assembly and cardiac function (Wang et al., 2001). These results

Correspondence to Anders Arner: anders.arner@ki.se

Abbreviations used in this paper: dpf, days postfertilization; GAPDH, glyceraldehyde 3-phosphate dehydrogenase; MO, morpholino antisense oligonucleotide; RT-PCR, reverse transcription PCR.

The Rockefeller University Press
J. Gen. Physiol. Vol. 141 No. 3 335–345
www.jgp.org/cgi/doi/10.1085/jgp.201210915

TABLE 1

Desmin genes, mRNA, splicing and translation blocking MOs

Criteria	*D. rerio, desma*	*D. rerio, desmb*
Zebrafish Model Organism Database (ZFIN) ID	ZDB-GENE-980526-221	ZDB-GENE-061027-102
mRNA	NM_130963.1	NM_001077452.1
Splice blocking	5′-AGATGACATAAAGTACATACAGCTC-3′	5′-TTTTGGTTTAGGACACTCACAGCTC-3′
Translation blocking	5′-CGGAGGCTGAATATTTCGTGCTCAT-3′	5′-GCTCATGTTGGAGCGATCAGATGAA-3′

The table shows the ZFIN (http://zfin.org)-entry for the gene, the mRNA entry (http://www.ncbi.nlm.nih.gov/), and the sequence for the splicing and translational morpholino oligonucleotides.

support the idea that the lack of normal desmin intermediate filaments is a key component in the alterations of structure and function of the contractile system in desminopathy. Much of our current mechanistic knowledge on desmin and intermediate filament function is obtained from desmin knockout mice (Li et al., 1996, 1997; Milner et al., 1996). These animals, with a complete ablation of desmin, are viable, but exhibit a myopathy affecting all muscle types. Key features of the skeletal muscle in the desmin knockout mice include structural changes in the myofibrillar integrity, lowered contractile strength, wider interfilament spacing, and altered sensitivity to acute stretch-induced injury (Sam et al., 2000; Wieneke et al., 2000; Balogh et al., 2003; Balogh et al., 2005). In addition, altered contractile function of cardiac and smooth muscle from the desmin knockout mice has been described previously (Sjuve et al.,1998; Balogh et al., 2002). It should be noted that the mouse desmin knockout model does not reveal any major pathological changes in the heterozygous animals, although the desmin protein content is lowered (Milner et al., 1996; Li et al., 1997), which might suggest that a complete suppression of desmin is required for a pathological muscle phenotype in the mouse.

To obtain mechanistic data on the structure–function relationship of desmin and related myofibrillar proteins in striated muscle, we have initiated an approach using physiology and structural studies of zebrafish larval muscle (Dou et al., 2008). The zebrafish (*Danio rerio*) is a vertebrate with several unique features as a model organism in science. The zebrafish genome is fully sequenced; homologues of human genes can be identified and specifically knocked down using morpholino antisense oligonucleotide (MO) injections. In addition, the animals can be maintained and bred in large quantities, are transparent in the larval stage, and develop most organ functions (including muscle) within a few days after fertilization. In our approach, we focus on the early larval stages (<6 d postfertilization [dpf]), accessible for oligonucleotide antisense knockdown, but still enabling quantitative analyses of muscle function. The main objective of this study was to develop a novel myopathy model with lowered desmin content in the zebrafish larvae and to analyze structural and functional alterations. We report that a partial removal of desmin results in a clear pathological muscle phenotype with distinct functional alterations in the zebrafish larvae, including altered active force generation, interfilament spacing, and sensitivity to stretch-induced injury. We could thus dissect the relative roles of lowered desmin versus pathological aggregates in affecting muscle function in desminopathy.

MATERIALS AND METHODS

Animals and preparation

Zebrafish embryos and larvae of the AB strain were obtained from the Karolinska Institutet zebrafish facility in the Department of Cell and Molecular Biology. The fish were held and raised at 28°C in a standard aquarium system (Schwarz Aquarienbau) using a 10–14-h dark-to-light cycle. Eggs were obtained using natural mating and MO injections were made in 1–2-cell-stage embryos. The larvae used in this study were 4–6 dpf. They were anesthetized using 0.017% MS-222 (tricaine methanesulfonate; Sigma-Aldrich) in E3 water (in mM: 5 NaCl, 0.17 KCl, 0.33 $CaCl_2$, and 0.33 $MgSO_4$) before mounting for mechanical or x-ray diffraction experiments or for fixation and biochemical and morphological analyses. The experiments were performed according to European guidelines for animal research, complied with national regulations for the care of experimental animals, and were approved by the local animal ethics committee.

Design and injection of MOs

In zebrafish, the *desmin* gene is duplicated on two chromosomes (*desma*: chromosome 9 and *desmb*: chromosome 6). We identified the two desmin genes (*desma* and *desmb*) in the zebrafish genome and obtained translation and splicing blocking MOs (Gene Tools LLC) as shown in Table 1. For comparison, we used a standard control MO (5′-CCTCTTACCTCAGTTACAATTTATA-3′; Gene Tools LLC). The embryos were injected with ∼5 nL, giving ∼4 ng of each MO, as further detailed in Results.

Reverse transcription PCR (RT-PCR) and Western blotting

RT-PCR was used to determine the extent of knockdown after injection of splicing blocking MOs. The RNA was extracted from dissected somite regions (removing head, gut, and heart) of individual 4 dpf larvae (RNeasy kit; QIAGEN), reverse transcribed (QuantiTect Reverse Transcription kit; QIAGEN), and amplified using the following forward (*desma*, 5′-ATCAGAGATCCCGTGTGGAG-3′; *desmb*, 5′-GACAACCTGGCAGATGACCT-3′) and reverse (*desma*, 5′-CCCTCGATACGTCTTTCCAG-3′; *desmb*, 5′-GGACTTGGGTCTCTTGCATC-3′) primers. *D. rerio* β-actin was used as a standard (forward, 5′-CCCAGACATCAGGGAGTGAT-3′; reverse, 5′-TCTCTGTTGGCTTTGGGATT-3′). The PCR products were analyzed on 2% agarose gels and the bands visualized using GelRed Nucleic Acid Gel Stain (Biotium) on a Bio-Rad system (Bio-Rad Laboratories).

Proteins were extracted from the somite regions using a homogenization buffer (composition in mM: 137 NaCl, 1 $MgCl_2$, 0.5 Na_3VO_4, 20 Tris, pH 7.8, 0.2 PMSF, 10 NaF, 5 sodium pyrophosphate, inhibitor cocktail [EMD Millipore], 1% Triton X-100, and 10% glycerol), mixed with SDS containing separation buffer, boiled for 5 min, centrifuged, and separated on 10% polyacrylamide gels. Extracts from 15 larvae (4 dpf, control injected or MO injected) were loaded on each lane. Protein bands were transferred to nitrocellulose membranes and incubated with rabbit polyclonal anti-desmin (ab86083; Abcam) and anti– glyceraldehyde 3-phosphate dehydrogenase (anti-GAPDH; sc-25778; Santa Cruz Biotechnology, Inc.) antibodies. ECL Western Blotting Detection Reagents (GE Healthcare), photographic film (Fuji), and optical scanning were used to quantify the desmin and GAPDH.

Analysis of swimming pattern and morphology

An automated behavioral analysis system, ZebraLab V3 (ViewPoint Life Sciences Inc.), for tracking larval swimming was used to assay the motility of control- and MO-injected larvae in E3 water at 25°C. The system records the large movements during 60 s with the following parameters: lardur (total duration spent by the animal in large movements), lardist (the total distance covered by the animal in large movements), and the calculated speed. For general morphology, the larvae were anesthetized and observed via light microscopy or euthanized and fixed in paraformaldehyde (4%, overnight at 4°C) in PBS, rinsed several times in PBS with 1% Triton X-100, treated with acetone (10 min at −20°C), rinsed, permeabilized with Trypsin (0.25%, 1–2 min on ice), stained with rhodamine phalloidin (1:40; Invitrogen), and imaged using a confocal microscope (LSM 510; Carl Zeiss). In one series of experiments, the larvae were fixed in glutaraldehyde (5% in 100 mM cacodylate buffer, pH 7.4, overnight), embedded in Araldite, sectioned, and analyzed with phase-contrast microscopy using the LSM 510 microscope.

X-ray diffraction

Small angle x-ray diffraction was used to determine the interfilament distances in the zebrafish larvae, as described previously (Dou et al., 2008), at beamline A2 at the Hamburger Synchrotronstrahlungslabor (HASYLAB)/Deutsches Elektronen-Synchrotron (DESY) synchrotron facility in Hamburg, Germany, and the beamline I911-SAXS at the MAX II ring of the MAX IV Laboratory in Lund, Sweden (Labrador et al., 2013). The larvae were euthanized and mounted horizontally using aluminum clips between two hooks in a Kapton cuvette in MOPS buffered physiological solution (in mM: 118 NaCl, 24 MOPS, 5 KCl, 1.2 $MgCl_2$, 1.2 Na_2HPO_4, 1.6 $CaCl_2$, and 10 glucose, pH 7.4) at 22°C and stretched to the optimal length for active force (L_{opt}, see "Mechanical analysis"), giving a sarcomere length of 2.1–2.2 µm confirmed by using HeNe laser diffraction. The MOPS buffered solution had an osmolarity of 271 mOsm. Solutions with different osmolarities were obtained by reducing NaCl (lowered osmolarity) or adding sucrose (higher osmolarity) to the MOPS buffered solution. Osmolarities of each solution were confirmed with direct osmometer measurements. For analysis of diffraction patterns in living and nonstretched preparations, the larvae were anesthetized with tricaine and kept in E3 medium, and in some experiments in the MOPS buffered solution, in a cuvette with Kapton windows. The camera length was 291.5–298.5 cm (HASYLAB) or 230 cm (MAX IV Laboratory). The diffraction patterns were recorded using a MarCCD camera (Marresearch GmbH) at HASYLAB or a PILATUS 1M detector (DECTRIS Ltd.) at MAX IV Laboratory. Calibrations of x-ray patterns were made using diffraction from rat tail collagen.

Mechanical analysis

Larval preparations were mounted as described above using aluminum clips between a force transducer and a puller for rapid length changes (Edman, 1999). The bath was perfused at 22°C with a Krebs buffered solution (in mM: 108 NaCl, 4.7 KCl, 1.2 $MgCl_2$, 1.2 KH_2PO_4, 35 $NaHCO_3$, 5.5 glucose, and 2.5 $CaCl_2$; osmolarity of 281 mOsm) gassed with 95% O_2 and 5% CO_2 to give a pH of 7.4. The preparations were mounted at slack length and then stimulated (single twitches) with 0.5-ms electrical pulses (supramaximal voltage) at 2-min intervals via two platinum electrodes placed on both sides of the preparation. Length was increased in steps between the contractions, from the slack length to a length above the maximal for active force. At each length, active and passive tensions were recorded. This length–tension relationship was determined for each preparation to identify the optimal length (L_{opt}). In a separate series on muscles stretched to L_{opt}, the effects of altered osmolarity were examined. Three single-twitch contractions were recorded at each osmolarity, and the average value was taken as representative. To examine the effects of stretch during active contractions, the muscles were stimulated at L_{opt} with 200 ms tetani (200 Hz) at 5-min intervals. A length ramp (10% stretch, at a rate of 2 L_{opt}/s) was imposed after 60 ms during the tetanus. The muscles were kept at the longer length for 200 ms and returned to L_{opt} in the relaxed state after the contractions. This stretch protocol is illustrated in the original recording shown in Fig. 5 C. In control experiments, the 200 ms tetani were repeated at 5 min intervals without stretch, i.e., isometric contractions (Fig. 5 A).

Statistics

All data are presented as mean ± SEM. Statistical analysis and curve fitting were performed using Sigma plot 8.0 for Windows and SigmaStat for Windows 3.0 (Systat Software, Inc.).

RESULTS

Effects of MO injection on desmin expression

We designed four MOs to block both splicing and translation of each desmin gene (Table 1). The splice-blocking MOs target the exon 2–intron 2 junction in the two zebrafish desmin genes, *desma* and *desmb*, respectively. Fig. 1 A shows RT-PCR results from individual 4-dpf larva. Transcripts (Fig. 1 A, arrows with solid lines) are identified in the control MO-injected larva, using primers for *desma* (Fig. 1 A, lane b; size 181 bp) and *desmb* (Fig. 1 A, lane e, size 238 bp). Similar results were obtained in noninjected wild-type larvae (unpublished data). These results thus show that both *desma* and *desmb* are expressed in muscles of 4-dpf larvae. To knock down both desmin isoforms we used a 50:50 mixture of the two MOs (*desma* + *desmb*), keeping the total amount of oligonucleotides at ∼3.75 ng, which is considered to be below the level causing unspecific effects (Bill et al., 2009). The mRNA expressions of both *desma* and *desmb* are significantly knocked down by a combination of *desma* and *desmb* MOs (Fig. 1 A, lane c and f), compared with the expression after control MOs injection. The expression of β-actin is slightly lowered after desmin MO injection (Fig. 1 A, lane i). As the splicing MOs target the exon–intron junction, we expect deletion of exon 2 (61 bp) of desmin pre-mRNA. We identified a transcript (Fig. 1 A, arrow with broken line, size ∼120 bp) reflecting the alternatively spliced mRNA. In control experiments, injection was performed

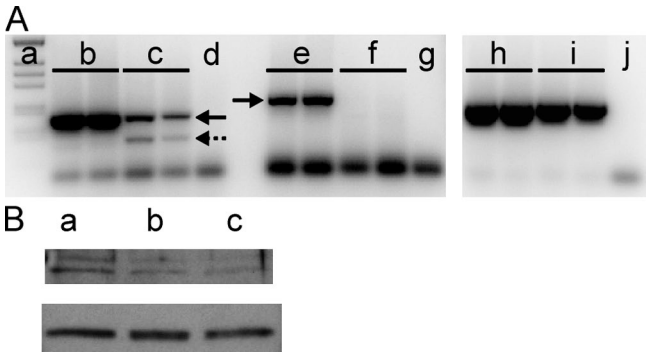

Figure 1. RT-PCR and Western blotting analyses of desmin in 4-dpf larvae. (A) A 2% agarose gel separation of standard (lane a; from the top: 506, 396, 344, 298, 220, and 201 bp) and of PCR products using primers for *desma* (lanes b–d) and *desmb* (lanes e–g). Lanes c and f show results from larvae injected with splice-blocking MOs for *desma* and *desmb* (50:50 with a total of ~3.75 ng); lanes d, g, and j are blank with primers only. Samples from control-injected larvae are shown in lanes b and e. The arrows indicate the main PCR products for *desma* and *desmb*. The broken arrow shows an extra PCR product for *desma* generated by the splicing process. Lanes h–j show corresponding PCR products on the same larval materials, using primers for β-actin. Each lane was loaded with extracts from a single larva. (B) Western blotting of desmin (top) and GAPDH (bottom) of extracts from control-injected (a), splice-blocking (b), and translation-blocking (c) MO-injected larvae. Extracts from 15 larvae were pooled and loaded in each lane.

using the respective splice-blocking MOs (~3.75 ng) targeting each individual gene isoform. This resulted in a specific knockdown of the individual gene without affecting the other isoform, showing that the MOs targeted selectively. However, when we injected a combination of the two MOs in this amount (i.e., 2 × 3.75 ng), a large population (>85%) of the larvae did not survive beyond 24 h, which suggests that the total amount of MOs was too high and caused off-target effects. Thus, we routinely used a combination of both MOs with a total amount of ~3.75 ng. For translation-blocking MOs we also used the 50:50 combination of both *desma* and *desmb* isoforms and the same total amount as for the splice-blocking MOs (~3.75 ng). The larvae injected with blocking MOs are denoted morphants in the subsequent text.

To also demonstrate knockdown at the protein level, we used Western blotting analyses on extracts from larvae (injected with control, splice-blocking, and translation-blocking MOs). The desmin gel band was visualized and normalized to GAPDH. Data are shown in Fig. 1 B. Extracts from 15 larvae in each group were used for each sample. The staining intensity of the GAPDH band was ~30% lower in larvae injected with blocking MOs (splicing, 73 ± 8%, $P < 0.05$; translation, 70 ± 14%, $n = 2–3$) compared with the control-injected larvae, reflecting the smaller size of the morphants. The desmin protein amount was significantly lower in the morphants blocked with splice- or translation-blocking MOs when normalized to the GAPDH level (splicing, 58 ± 5%, $P < 0.05$; translation, 44 ± 4%, $n = 2–3$). These results show that injection of splice- or translation-blocking MOs results in smaller larvae (less GAPDH), but also a significant (by ~50%) specific lowering of the desmin protein in the 4-dpf larvae muscle.

Larval phenotype and morphology

The general characteristics of the larvae are shown in Table 2. Injected larvae (controls and desmin morphants) had a somewhat lower general survival rate, but the desmin morphants were more severely affected compared with the control-injected samples. The hatching rate at 3 dpf was also lower in the desmin morphants, which might indicate weaker muscle strength. The body length at 4 dpf was ~10% shorter in the morphants. We performed a motion analysis on control and splicing morphant larvae (Table 2). Whereas the controls moved constantly during the 60-s recording period, the

TABLE 2

General characteristics of wild-type larvae, and larvae injected with control, splice-blocking, and translation-blocking MO

Criteria	Wild type	Control	Splicing MO	Translation MO
Survival rate (%)	>95	74 ± 7	47 ± 7[a]	48 ± 5[a]
Hatching rate (%)	>85	86 ± 3	47 ± 7[b]	42 ± 7[b]
Body length (mm)	3.6 ± 0.13	3.6 ± 0.04	3.2 ± 0.06[b]	3.04 ± 0.11[b]
lardur (s)		60	22 ± 9[d]	
lardist (cm)		141 ± 13	36 ± 19[d]	
Speed (cm/s)		2.4 ± 0.2	1.2 ± 0.5[c]	

The mean values in the table are calculated as mean rates of 24 hpf (hour postfertilization) survival and 3 dpf hatching (among the surviving eggs), determined in three independent injection rounds (each comprising 50–100 eggs). Body length was measured at 4 dpf, from the snout to the posterior end of the larval body. The measurements of swimming behavior of 4-dpf controls ($n = 10$) and desmin-splicing morphants ($n = 7$) were recorded during 60 s. The lardur parameter is the mean time spent by larvae in large movements, lardist is the distance covered by larvae during large movements, and speed is calculated by lardist/lardur.

[a]Significant difference ($P < 0.05$) compared with the control group (ANOVA, using the Holm-Sidak method).

[b]Significant difference ($P < 0.01$) compared with the control group (ANOVA, using the Holm-Sidak method).

[c]Significant difference ($P < 0.05$) compared with the control group (Student's *t* test).

[d]Significant difference ($P < 0.001$) compared with the control group (Student's *t* test).

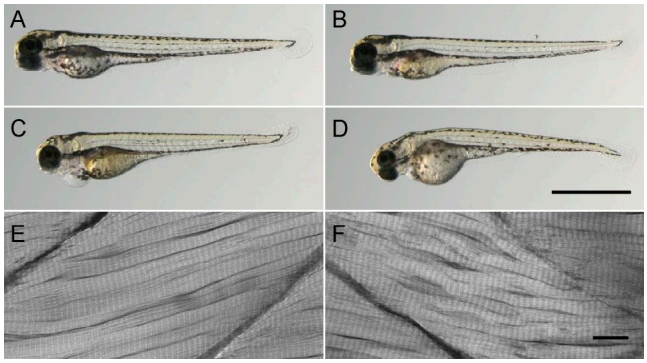

Figure 2. Morphology of control and morphant larvae. Microscopy photographs of 4-dpf wild-type (A) and control-injected (B) larvae. (C and D) Splice- and translation-blocking MO-injected morphants, respectively. Both types of morphants had signs of cardiac edema. (E and F) Confocal microscopy of a control (E) and a splicing morphant (F) stained with rhodamine phalloidin. Bars: (A–D) 1 mm; (E and F) 10 μm.

morphants spent only about one third of the time swimming and moved with a lower speed. Fig. 2 shows representative microscopy pictures of the different larval groups at 4 dpf. Both types of morphants were shorter, with a slightly bent phenotype and with signs of edema surrounding the heart. The lower panels in Fig. 2 show corresponding confocal microscopy pictures of whole-mount preparations stained with rhodamine phalloidin to visualize actin. As seen in the microscopy pictures, the control muscle fibers were well aligned with regular attachments to the myosepta. In contrast, the morphant muscles were disorganized, with small gaps between the muscle fibers and areas with disorganized fibers. The area with gaps was evaluated by measuring the intensity under a 40-μm line scan in the middle of the somite in the rhodamine phalloidin stained samples. The relative area with gaps was significantly larger in the morphants (controls, 10 ± 0.7%; morphants, 13 ± 0.7%, $P < 0.05$), which would correspond to an ∼7% smaller cross-sectional area of the muscle in the somites. The myosepta also appeared thinner, with less distinct periodic patterns. In some regions, the attachment sites for the muscle fibers to the myosepta were altered in the morphants compared with the controls. In both controls and morphants, the sarcomere patterns were clearly visible and regular, with a similar sarcomere length (∼1.7 μm) in the two groups under these conditions. Phase-contrast microscopy of the larvae fixed in glutaraldehyde revealed that the desmin morphants had an ∼15% shorter somite length (78.7 ± 0.8 vs. 91.3 ± 1 μm; $n = 2$).

Interfilament spacing

Small angle x-ray diffraction was used to examine the effects of desmin knockdown on sarcomeric structure. The equatorial patterns with the 1.0 and 1.1 reflections were well resolved in both controls and morphants (Fig. 3, A–C). These recordings were performed with the muscles stretched to optimal length (L_{opt}) as determined in the mechanical experiments (stretched by 30% from slack length L_s, see "Length–tension relationships"). The corresponding sarcomere length was confirmed with laser diffraction (2.1–2.2 μm) in samples of both controls and morphants. In both translation- and splice-blocking morphants, the interfilament spacing was significantly wider than that of the controls at optimal length (Fig. 3 E). When the muscles were examined in the slack/extended state (L_s, ∼80% of optimal length), the interfilament spacing (as evaluated from the 1.0 reflection) was wider compared with that at L_{opt} in all groups. Also under this condition, the desmin morphants were slightly

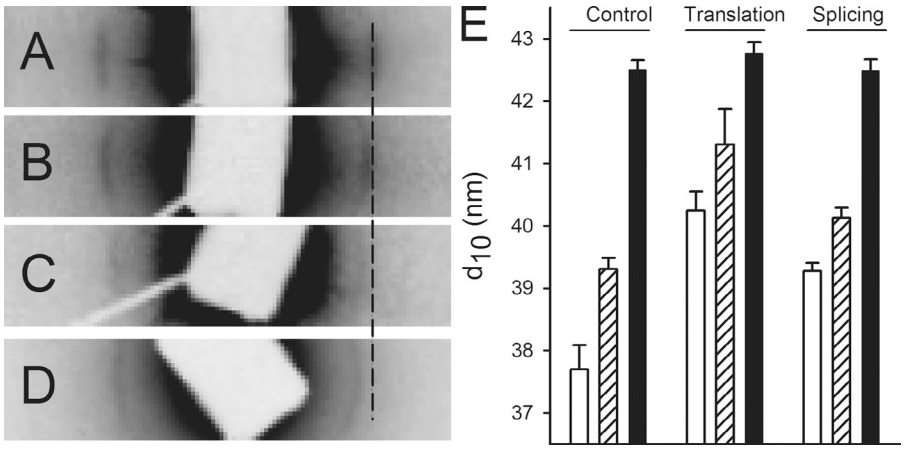

Figure 3. X-ray diffraction of control and morphant larvae. The equatorial region of small angle x-ray diffraction patterns recorded from control-injected (A) and splice- and translation-blocking morphants (B and C) at 4 dpf. The muscles were mounted at optimal length (L_{opt}). The equator in the pattern is oriented horizontally, and the position of the 1.0 reflection (corresponding to 37.9 nm) in the control is indicated with a broken line. (D) A recording from a living, anesthetized control larva in E3 medium. (E) The spacing of 1.0 reflection in the different groups at L_{opt} (open bars, sarcomere length 2.1–2.2 μm), slack (L_s, hatched bars, ∼1.7 μm), and in a living state (shaded bars). Statistical analysis ($n = 3$–6 in each group, $P < 0.05$; one-way ANOVA, and Holm-Sidak method for multiple comparisons) revealed that shortening (L_{opt} vs. L_s) gives a significant increase ($P < 0.05$) in spacing of controls and translation-blocking morphants. Living larvae had a wider spacing in all groups compared with mounted larvae (at L_s or L_{opt}). Morphants (translation and splicing) had a wider spacing than controls at L_{opt} and for translation also at L_s. No differences were detected between the living larval groups. Error bars indicate mean ± SEM.

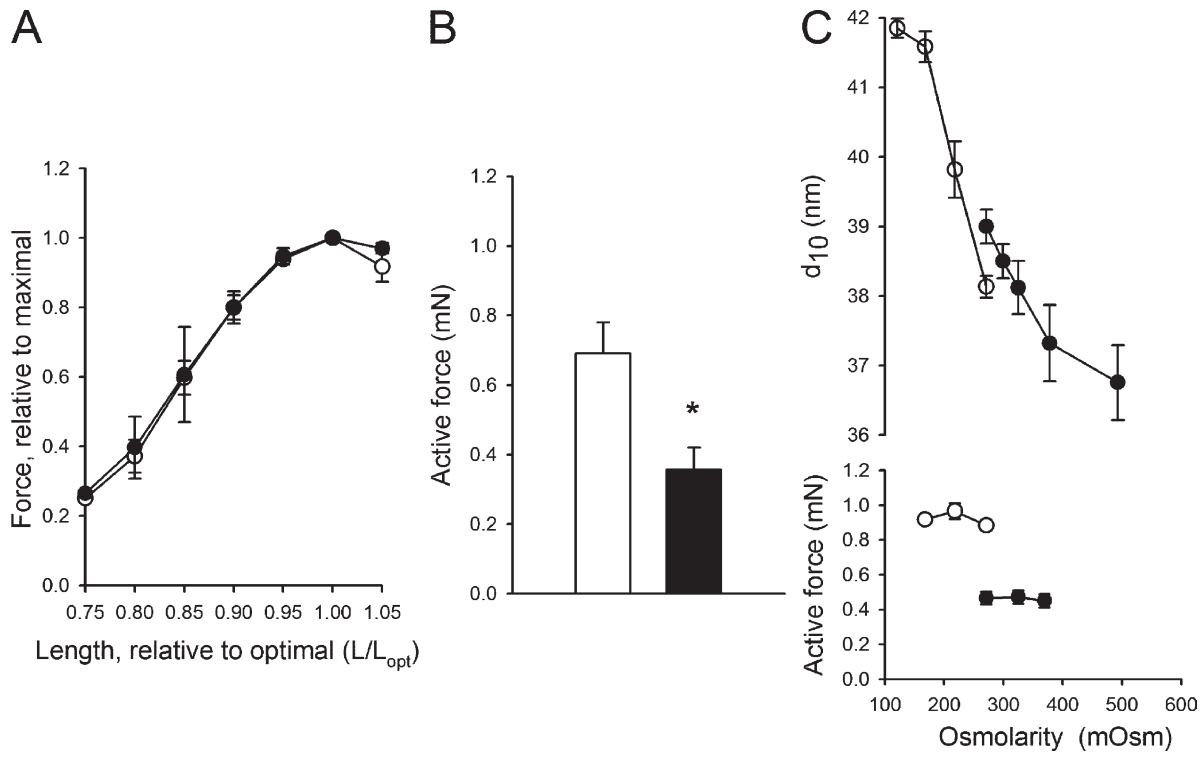

Figure 4. Length–tension relationship and maximal active force in skeletal muscles. Data from 4-dpf control (open symbols) and desmin morphant (closed symbols) zebrafish larvae are shown. Muscles were stimulated to give single twitches. (A) Force and length values are given relative to the respective values at optimal length (L_{opt}). (B) The maximal active force at L_{opt} is presented. $n = 6$; *, $P < 0.05$. (C) The equatorial 1.0 spacing (top) and active force (bottom) of the muscles at L_{opt} examined at different osmolarities. Control (open symbols) and desmin morphants (closed symbols) are shown, $n = 4$ in each group. Error bars indicate mean ± SEM.

wider compared with the controls. In the living nonmounted larvae in E3 medium (Figs. 3 D and Fig. 3 E, filled bars), the interfilament spacing was wider than that of the muscles mounted (at L_s or L_{opt}) in the MOPS buffered solution. To further examine if the wider spacing in the living larvae muscles was caused by the lower osmolarity in the E3 medium, we compared 6-dpf living control larvae in E3 and MOPS buffered solutions. The sarcomere length of the living 6-dpf anesthetized larvae was 1.76 µm in E3 medium. Although the 1.0 equatorial spacing in this series was somewhat more narrow than that shown in Fig. 3 on 4-dpf larvae, no difference was detected (MOPS, 40.4 ± 0.31; E3, 40.8 ± 0.05 nm, $n = 5$–6), showing that the external osmolarity does not have a major impact on lattice spacing in the living larvae. In summary, the x-ray diffraction experiments revealed that stretch results in a decreased interfilament spacing. The morphants have a wider spacing at optimal length and are less affected by stretching. In the living nonstretched larvae, the spacing was wider than isolated preparations at L_{opt} and similar in all groups.

Length–tension relationships

The length–tension relationship was determined in 4-dpf control and morphant (splicing) muscles, stimulated with single pulses at different lengths. The relationship (Fig. 4 A) was bell-shaped with an optimal length (L_{opt}) when the muscle was stretched by 30% (controls, 30 ± 1%, $n = 10$; morphants, 29 ± 2%, $n = 8$) from the slack length (L_s) recorded after mounting. The relationships were similar in controls and morphants, when force was normalized to maximal. The sarcomere length was determined using laser diffraction in a set of muscles ($n = 6$) stretched to L_{opt}, and we confirmed that the value was in the range 2.1–2.3 µm, which is close to that reported previously for 7-dpf larvae (Dou et al., 2008). The passive tension at L_{opt} did not differ between the two groups (controls, 0.078 ± 0.013 mN, $n = 8$; morphants, 0.071 ± 0.018 mN, $n = 5$). The active force at optimal length (Fig. 4 B) was ∼50% lower in the splicing morphants ($P < 0.05$). Because the larval preparations have a comparatively complex organization of muscle and other tissue components, we could not accurately determine the cross-sectional area. However, we measured the thickness (in transverse direction) of the larvae at the widest position (between somites 12 and 16) at slack length in MOPS buffered medium, and found a slightly thinner diameter in morphants (controls, 0.243 ± 0.002 mm; morphants, 0.239 ± 0.003 mm). Using the shape of the muscle components at this somite position at this developmental stage

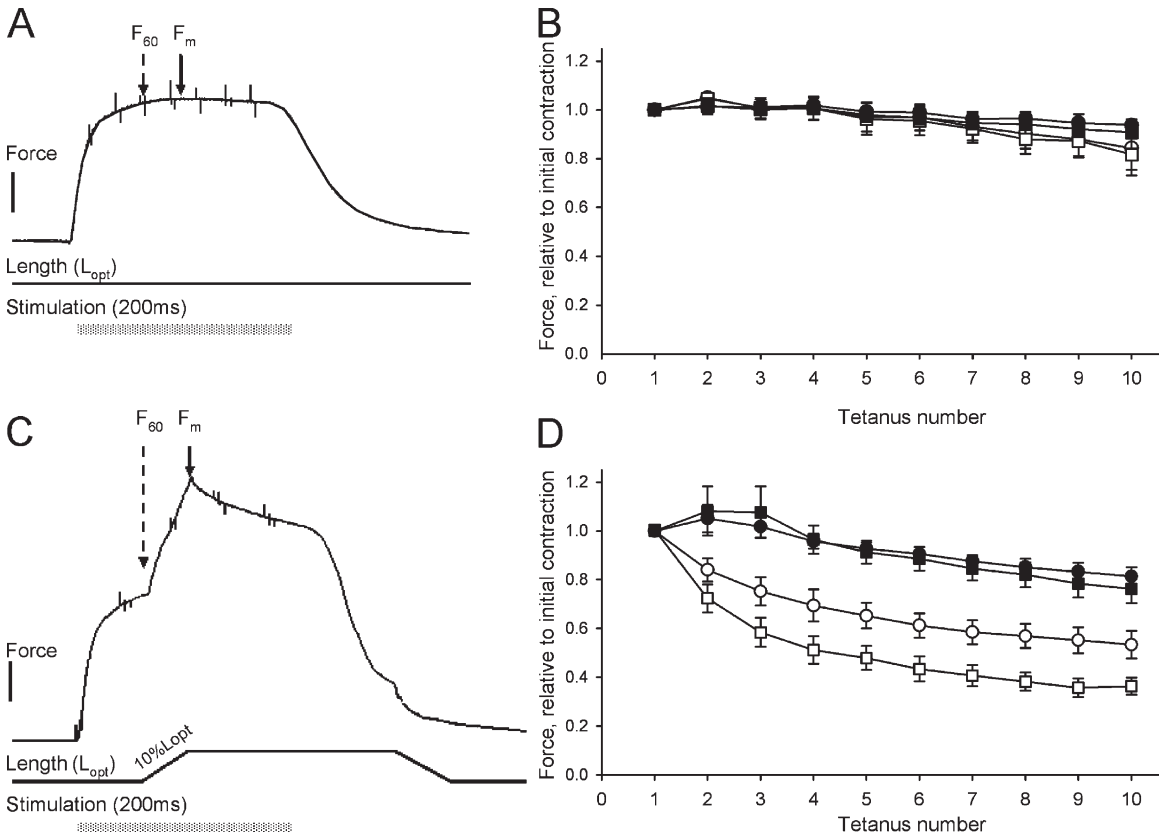

Figure 5. Stretch-induced effects on active force. A and C show original recordings of length and active force of 4 dpf control larvae stimulated during 200 ms with 200 Hz at optimal length. The contraction in A was isometric and the contraction in C involved a 10% stretch ramp (rate: 2 L_{opt}/s) imposed 60 ms after onset of activation. Muscle length was returned to optimal 60 ms after cessation of the stimulation. The force at 60 ms after activation (F_{60}), before the onset of the stretch ramp, and the maximal force (F_m) were evaluated. Force scale bar, 0.2 mN. The right panels show the contractile responses in muscles kept isometric (B, compare with A), or stretched (D, compare with C). F_{60} (squares) and F_m (circles) values were normalized to the initial responses during the first contraction. The experiments were performed on control (open symbols, $n = 11$) and splicing morphants (closed symbols, $n = 6$). The force responses (F_m and F_{60}) of the splicing morphants were significantly ($P < 0.001$, one-way ANOVA and Holm-Sidak method) higher than the corresponding values in the control group during at the final 10th contraction of the stretch experiments (D). Error bars indicate mean ± SEM.

(http://fishnet.med.monash.edu.au/index.shtml) and our measurements of the larval thickness, we estimated the cross-sectional area at the widest position in controls and morphants to 0.031 ± 0.006 and 0.027 ± 0.006 mm^2, respectively. The ∼13% smaller cross-sectional area can thus explain in part the lower active force, but because the active tension was ∼50% lower, it is likely that an additional effect of knockdown lowers the active force in the morphants.

In a separate series of experiments, we addressed the question of whether a wider spacing in the desmin morphants can explain the decrease in active force. We therefore expanded the lattice spacing of the control muscles and compressed the morphants with altered osmolarity in the bathing solutions (Fig. 4 C). The altered tonicity had clear effects on the filament lattice spacing. In parallel, we examined the mechanical effects and found that the controls did not become weaker when expanded to the spacing of the morphants. Compression of the lattice in the morphants to the spacing of controls did not rescue the active force. These results thus show that the decreased force of the morphants is not caused by the wider interfilament spacing.

Responses to stretch during active contraction

To explore if the lowered desmin expression and altered muscle structure affect the responses to stretching and to stretch-induced decay of tension, we activated the muscles with short tetanic stimulations and imposed a 10% stretch ramp at the plateau (60 ms after onset of stimulation) of the contraction. The original recording in Fig. 5 A shows the contractile response to a 200-ms, 200-Hz tetanic stimulation. A fused and stable contraction developed. The sustained maximal tension (F_m) was on average 102 ± 1% ($n = 5$) of the force at 60 ms (F_{60}) in control muscles and 104 ± 2% ($n = 3$) in splicing morphants. This shows that the force was already very close to a plateau at 60 ms. No difference in the F_m/F_{60} values could be detected between the two groups, although the F_m values were significantly ($P < 0.05$) lower in the morphant group when expressed in absolute force

units (controls, 0.66 ± 0.01 mN, $n = 5$; morphants, 0.35 ± 0.06 mN, $n = 4$), similar to the values for single twitch (Fig. 4 B). These isometric contractions could be repeated with minor loss of force (both F_{60} and F_m) when the muscles were stimulated at 5-min intervals (Fig. 5 B). When the muscles were ramp-stretched by 10% at the plateau of the tetanus, a significant tension rise was observed (Fig. 5 C), reaching a level about twice that of nonstretched muscles (F_m/F_{60}; controls, 170 ± 4%, $n = 3$; morphants, 168 ± 7%, $n = 4$). During 10 successive stretches, both the F_{60} and the F_m tension values of the control preparations decayed significantly (Fig. 5 D, open symbols). At the 10th stimulus, the F_{60} tension had decayed by ∼60%. In contrast, the splicing morphants lost significantly less tension compared with controls when stimulated and stretched (Fig. 5 D, closed symbols). At the 10th stimulus, the F_{60} tension had decayed by ∼20%. These results show that the splicing desmin morphants have a significantly higher resistance to stretch-induced decay of tension.

DISCUSSION

We demonstrated expression of two desmin genes in the zebrafish larvae and used MOs to knock down ∼50% of the desmin in 4-dpf early larvae. Previous studies have shown that the desmin protein is similar to that of vertebrates (with 68.7% similarity to human desmin) and that the desmin expression in zebrafish can be detected at the 1–3-somite stage (Loh et al., 2000). Although the knockdown in our experiments was partial, significant structural and functional alterations were observed.

The general architecture of the somite muscles and the sarcomere patterns was preserved in the morphants. However, clear structural changes, including a disordering of muscle fibers with small gaps between the muscle fibers, were found. In addition, the intersomite junctions appeared thinner, with less distinct attachments of the muscle fibers. In some more affected areas (unpublished data), the muscle fibers had lost contact with the intersomite junctions. A previous study on the *Xenopus laevis* has shown that overexpression of truncated intermediate filament proteins leads to disruption of the myofibrillar membrane attachments and alterations in the intersomite junctions of the myotomal muscles (Cary and Klymkowsky, 1995). This suggests that the mutated proteins, or the lack of normal intermediate filament proteins, affect these attachment sites. Our data are consistent with these results and support the latter hypothesis that desmin is required for maintaining the intersomite junctions, in addition to maintaining lateral connections. Desmin most likely provides a mechanical link between the terminal Z-disks and the membrane attachment sites (Tidball, 1992), possibly also affecting the localization of other costamere-associated proteins (Carlsson et al., 2000).

Human desminopathies are usually associated with abnormal aggregates of desmin (Paulin et al., 2004; van Spaendonck-Zwarts et al., 2011). Because these human diseases do not have a complete lack of desmin, it is an open question whether the structural and functional defects are caused by toxic effects of the aggregates or to a loss of desmin. Significant information regarding the role of desmin in muscle has been obtained using desmin knockout mice (Li et al., 1996, 1997; Milner et al., 1996; Thornell et al., 1997). In this model, the heterozygous animals were not affected (Milner et al., 1996; Li et al., 1997), although the desmin content was reduced. This implies that a larger extent of desmin reduction (i.e., in the homozygous knockout mice) is required for structural and functional changes in the mouse muscles. The zebrafish desmin knockdown model, presented here, shows that a comparatively severe muscle phenotype can be caused by an ∼50% loss of desmin. This supports the hypothesis that a partial loss of desmin is sufficient to cause structural and functional alterations in the contractile apparatus in desminopathy. Although not the focus of the present study, we also found alterations in the heart of the zebrafish desmin morphants, similar to alterations previously reported from desmin knockout mice (Li et al., 1996; Milner et al., 1996), which suggests that desmin also has a structural role in other muscle organs of the zebrafish. Interestingly, the novel zebrafish desmin knockdown model enables studies of desmin effects on skeletal muscle function independent of potential interfering effects from heart and visceral organs, as the cardiac and gastrointestinal functions are not required for the early zebrafish development (Sehnert et al., 2002).

The intermediate filament system anchors muscle sarcomeres at the Z-lines, providing lateral contacts (Lazarides, 1980), and in the desmin knockout mouse a wider interfilament spacing has been reported for soleus muscle fibers (Balogh et al., 2005). We therefore hypothesized that the lack of desmin would affect the spacing and lateral force transduction between the contractile filaments in the zebrafish larval muscle. In the relaxed, nonstretched living larvae, where the muscle length is below optimal for active force, the filament lattice was comparatively wide and similar in controls and desmin morphants. This suggests that a general change of cellular architecture in the desmin morphants does not contribute to the lateral arrangement of the contractile filament. However, when the larvae were mounted at slack or optimal length in physiological buffer solution, the lattice became narrower, indicating a lateral compression of the sarcomere. The compression (living vs. mounted at slack length) cannot be simply explained by a change in solution osmolarity, as the E3 and MOPS buffered solutions gave similar filament spacing in living muscles. This can't be explained by a stretch of sarcomeres either, as the sarcomere lengths of preparations mounted at slack length

and living larvae muscle were similar. It is possible that a small extension of the muscles when mounting compresses the filament lattice without large changes in sarcomere length. Although the desmin morphants had similar filament spacing in the living state, they were less compressed when mounted at slack length and when stretched to optimal, compared with the controls. Thus, the partial removal of desmin affects the lateral compliance of the muscle fibers and influences the mechanical coupling of the sarcomere in the muscle cells. Importantly, the wider spacing in the morphants is most significant when the muscles are operating at optimal stretch. The mechanism by which desmin contributes to the maintenance of lattice spacing is presently unclear. However, studies of transgenic mice have suggested that lack of desmin leads to disorganization and eventually disintegration of the Z-discs (Li et al., 1997). The expansion of the lattice can thus be an early sign of impaired Z-disc structure or caused by the altered connections between adjacent myofibrils, affecting the packing of the contractile filaments. Although studies on mice have shown that titin expression is not altered in the desmin knockout animals (Anderson et al., 2002; Balogh et al., 2005), we cannot exclude the possibility that the knockdown of desmin in the zebrafish larvae affects the expression of other cytoskeletal proteins influencing myofibrillar structure.

Although zebrafish have been extensively examined from a developmental perspective focusing on structural aspects, functional data from zebrafish larval muscles are sparse. In a translational context, from an animal model to human muscle disease, information on contractile function is crucial and is a relevant indicator of the extent of pathological changes in the muscle. We therefore applied a mechanical analysis of the larval muscles (Dou et al., 2008) and report data from the 4-d-old larvae. The length–tension relationship was not affected in the desmin morphants, with an optimal sarcomere length similar to that in the controls, which is consistent with the generally preserved muscle fibers and sarcomere patterns. However, the active force was significantly lower, which in part was caused by the smaller size of the muscles, with a minor contribution from gaps between muscle fibers, but mainly to a specific effect on force generation. The mechanism for this is unclear. Studies of frog muscle fibers have shown that lowered tonicity of the bathing medium and the associated fiber swelling causes an increase in active force generation with a reduced stretch resistance (Edman, 1999). We show that compression of the filament lattice in the morphants could not rescue the active force; neither could expansion of the lattice in control fibers introduce a decreased active force. It is therefore unlikely that the swelling of the lattice is a primary cause for the reduction of active force in the morphant zebrafish larvae. The cytoskeleton has been shown to affect both mitochondrial functions and energy-dependent Ca^{2+} handling in cardiac muscle (Wilding et al., 2006). It is possible that alterations in these processes are involved in the lowered active tension of the desmin morphants, although the larval muscles are of a fast phenotype and most likely not critically dependent on aerobic ATP generation during the very short active contractions. Previous studies of desmin knockout mice have shown that active force is reduced, without changes in contractile protein content and excitation–contraction coupling (Sjuve et al., 1998; Balogh et al., 2002, 2003). This was suggested to reflect a misalignment and sarcomere length inhomogeneity during contraction in the absence of intermediate filaments. Altered three-dimensional mechanical properties and increased myofibrillar mobility have been described in desmin-deficient mouse skeletal muscles (Boriek et al., 2001; Shah et al., 2002), which is consistent with this hypothesis. Based on these mechanical considerations, we suggest that the partial removal of desmin in the zebrafish model reduces active tension at optimal length of the striated muscle via a structural mechanism. This might involve sarcomere length inhomogeneity during contraction or affected force transmission caused by a lack of mechanical coupling in the longitudinal and transverse directions.

From an animal physiology perspective, we note that the living larvae in the relaxed state have a sarcomere length that is significantly below optimal. One might speculate on the physiological significance of this. During escape responses with burst swimming ("C-start behavior"), the larvae bend the tail almost in a semicircle (Budick and O'Malley, 2000). During bending, the muscles at the outer circumference will be stretched, resulting in a compressed filament lattice, while opposite changes occur in the muscles at the inner circumference. Based on the structural and length–tension data, we predict that the outer muscles will be positioned close to the optimal length for active tension when the tail is bent. This will favor a powerful tail swing during which the inner muscles, if activated, have a lower active tension, due to the short sarcomere length, and less stretch resistance, due to the wider filament spacing.

To further explore the functional consequences of desmin knockdown in the larval skeletal muscles, we applied an eccentric contraction protocol where the muscles were stretched during tetanic contractions to induce an acute injury. Previous studies, using this protocol, have shown that muscles from desmin knockout mice are less vulnerable to mechanical injury (Sam et al., 2000). Our results from the zebrafish larvae with desmin knockdown are consistent with this. Because the relative force increase during the imposed stretch was similar in the morphants and the controls, the mechanical work performed on the muscles was not different. Nevertheless, the drop of active tension induced by the eccentric contractions was significantly lower in

the desmin morphants, which could relate to more compliant muscles. The resistance to stretch-induced injury in the desmin morphants can include many components affecting the impact of the eccentric work, e.g., an inhomogeneity of the stretch within the muscle fiber, or internal slippage caused by the wider spacing. In a previous study of frog skeletal muscles, swelling was associated with a lower stretch resistance (Edman, 1999), and an interesting possibility is that the swollen lattice in the desmin morphant larvae lowers the resistance to stretching in the sarcomere and thereby protects the sarcomeres from stretch-induced injury. It should be noted that the stretch rate and amplitudes used to induce injury (10% of the muscle length, with a stretch rate of 200%/s) were significantly higher than those applied to the frog fibers (2% at ∼20%/s; Edman, 1999) and thus a lowered stretch resistance might not be resolved during our stretch protocols. It is well known that dystrophic muscles are highly sensitive to stretch-induced injury (Petrof et al., 1993). Whether this observation from dystrophin-deficient muscles also extrapolates to desmin-related myopathy is unknown. Previous studies have shown effects of desmin on myoblast proliferation and muscle regeneration (Smythe et al., 2001). Our finding that the desmin-deficient muscles are less vulnerable to stretching in the acute situation therefore suggests that if stretch-induced injury occurs in desminopathy, it is a consequence of subsequent processes in degeneration or repair, rather than in an increased stretch sensitivity of the contractile components per se.

In summary, we present a novel zebrafish model of desmin-related myopathy with significant structural and functional alterations. The results show that a partial loss of desmin is sufficient to cause a clear muscle phenotype mimicking several aspects of human desminopathy. Functional studies showed a decreased active force and lower vulnerability to acute stretch induced injury. These changes are most likely associated with altered force transmission in the muscle and with structural changes in the sarcomeres caused by lowered content of desmin intermediate filaments.

We are very grateful and honored to have been able to use the mechanical equipment from Professor Paul Edman's laboratory and for his thoughtful and constructive suggestions on the manuscript. We appreciate the competent help with zebrafish handling and breeding from Mr. Kent Ivarsen (CMB zebrafish facility at Karolinska Institutet), and with preparations of muscle sections from Ms. Rita Wallén (Zoophysiology, Lund University). We are very grateful for the competent help from Dr. Sérgio S. Funari at the A2 beamline in HASYLAB, Hamburg Germany, and from Dr. Ana Labrador at the I911-SAXS beamline at Max IV Laboratory, Lund, Sweden.

This study was supported by grants from the Swedish Research Council (2009-4302), the Swedish Heart Lung Foundation (20080648), and the Association Française Contre les Myopathies (16304).

Richard L. Moss served as editor.

Submitted: 17 October 2012
Accepted: 29 January 2013

REFERENCES

Anderson, J., V. Joumaa, L. Stevens, C. Neagoe, Z. Li, Y. Mounier, W.A. Linke, and F. Goubel. 2002. Passive stiffness changes in soleus muscles from desmin knockout mice are not due to titin modifications. *Pflugers Arch.* 444:771–776. http://dx.doi.org/10.1007/s00424-002-0875-0

Balogh, J., M. Merisckay, Z. Li, D. Paulin, and A. Arner. 2002. Hearts from mice lacking desmin have a myopathy with impaired active force generation and unaltered wall compliance. *Cardiovasc. Res.* 53:439–450. http://dx.doi.org/10.1016/S0008-6363(01)00500-4

Balogh, J., Z. Li, D. Paulin, and A. Arner. 2003. Lower active force generation and improved fatigue resistance in skeletal muscle from desmin deficient mice. *J. Muscle Res. Cell Motil.* 24:453–459. http://dx.doi.org/10.1023/A:1027353930229

Balogh, J., Z. Li, D. Paulin, and A. Arner. 2005. Desmin filaments influence myofilament spacing and lateral compliance of slow skeletal muscle fibers. *Biophys. J.* 88:1156–1165. http://dx.doi.org/10.1529/biophysj.104.042630

Bill, B.R., A.M. Petzold, K.J. Clark, L.A. Schimmenti, and S.C. Ekker. 2009. A primer for morpholino use in zebrafish. *Zebrafish.* 6:69–77. http://dx.doi.org/10.1089/zeb.2008.0555

Boriek, A.M., Y. Capetanaki, W. Hwang, T. Officer, M. Badshah, J. Rodarte, and J.G. Tidball. 2001. Desmin integrates the three-dimensional mechanical properties of muscles. *Am. J. Physiol. Cell Physiol.* 280:C46–C52.

Budick, S.A., and D.M. O'Malley. 2000. Locomotor repertoire of the larval zebrafish: swimming, turning and prey capture. *J. Exp. Biol.* 203:2565–2579.

Carlsson, L., Z.L. Li, D. Paulin, M.G. Price, J. Breckler, R.M. Robson, G. Wiche, and L.E. Thornell. 2000. Differences in the distribution of synemin, paranemin, and plectin in skeletal muscles of wild-type and desmin knock-out mice. *Histochem. Cell Biol.* 114:39–47.

Cary, R.B., and M.W. Klymkowsky. 1995. Disruption of intermediate filament organization leads to structural defects at the intersomite junction in *Xenopus* myotomal muscle. *Development.* 121:1041–1052.

Dalakas, M.C., K.Y. Park, C. Semino-Mora, H.S. Lee, K. Sivakumar, and L.G. Goldfarb. 2000. Desmin myopathy, a skeletal myopathy with cardiomyopathy caused by mutations in the desmin gene. *N. Engl. J. Med.* 342:770–780. http://dx.doi.org/10.1056/NEJM200003163421104

Dou, Y., M. Andersson-Lendahl, and A. Arner. 2008. Structure and function of skeletal muscle in zebrafish early larvae. *J. Gen. Physiol.* 131:445–453. http://dx.doi.org/10.1085/jgp.200809982

Edman, K.A. 1999. The force bearing capacity of frog muscle fibres during stretch: its relation to sarcomere length and fibre width. *J. Physiol.* 519:515–526. http://dx.doi.org/10.1111/j.1469-7793.1999.0515m.x

Ferrer, I., and M. Olivé. 2008. Molecular pathology of myofibrillar myopathies. *Expert Rev. Mol. Med.* 10:e25. http://dx.doi.org/10.1017/S1462399408000793

Labrador, A., Y. Cerenius, C. Svensson, K. Theodor, and T. Plivelic. 2013. The yellow mini-hutch for SAXS experiments at MAX IV Laboratory. *J. Phys. Conf. Ser.* In press.

Lazarides, E. 1980. Intermediate filaments as mechanical integrators of cellular space. *Nature.* 283:249–256. http://dx.doi.org/10.1038/283249a0

Li, Z., E. Colucci-Guyon, M. Pinçon-Raymond, M. Mericskay, S. Pournin, D. Paulin, and C. Babinet. 1996. Cardiovascular lesions

and skeletal myopathy in mice lacking desmin. *Dev. Biol.* 175:362–366. http://dx.doi.org/10.1006/dbio.1996.0122

Li, Z., M. Mericskay, O. Agbulut, G. Butler-Browne, L. Carlsson, L.E. Thornell, C. Babinet, and D. Paulin. 1997. Desmin is essential for the tensile strength and integrity of myofibrils but not for myogenic commitment, differentiation, and fusion of skeletal muscle. *J. Cell Biol.* 139:129–144. http://dx.doi.org/10.1083/jcb.139.1.129

Loh, S.H., W.T. Chan, Z. Gong, T.M. Lim, and K.L. Chua. 2000. Characterization of a zebrafish (*Danio rerio*) desmin cDNA: an early molecular marker of myogenesis. *Differentiation.* 65:247–254. http://dx.doi.org/10.1046/j.1432-0436.2000.6550247.x

Milner, D.J., G. Weitzer, D. Tran, A. Bradley, and Y. Capetanaki. 1996. Disruption of muscle architecture and myocardial degeneration in mice lacking desmin. *J. Cell Biol.* 134:1255–1270. http://dx.doi.org/10.1083/jcb.134.5.1255

Muñoz-Mármol, A.M., G. Strasser, M. Isamat, P.A. Coulombe, Y. Yang, X. Roca, E. Vela, J.L. Mate, J. Coll, M.T. Fernández-Figueras, et al. 1998. A dysfunctional desmin mutation in a patient with severe generalized myopathy. *Proc. Natl. Acad. Sci. USA.* 95:11312–11317. http://dx.doi.org/10.1073/pnas.95.19.11312

Paulin, D., A. Huet, L. Khanamyrian, and Z. Xue. 2004. Desminopathies in muscle disease. *J. Pathol.* 204:418–427. http://dx.doi.org/10.1002/path.1639

Petrof, B.J., J.B. Shrager, H.H. Stedman, A.M. Kelly, and H.L. Sweeney. 1993. Dystrophin protects the sarcolemma from stresses developed during muscle contraction. *Proc. Natl. Acad. Sci. USA.* 90:3710–3714. http://dx.doi.org/10.1073/pnas.90.8.3710

Sam, M., S. Shah, J. Fridén, D.J. Milner, Y. Capetanaki, and R.L. Lieber. 2000. Desmin knockout muscles generate lower stress and are less vulnerable to injury compared with wild-type muscles. *Am. J. Physiol. Cell Physiol.* 279:C1116–C1122.

Schröder, R., and B. Schoser. 2009. Myofibrillar myopathies: a clinical and myopathological guide. *Brain Pathol.* 19:483–492. http://dx.doi.org/10.1111/j.1750-3639.2009.00289.x

Sehnert, A.J., A. Huq, B.M. Weinstein, C. Walker, M. Fishman, and D.Y. Stainier. 2002. Cardiac troponin T is essential in sarcomere assembly and cardiac contractility. *Nat. Genet.* 31:106–110. http://dx.doi.org/10.1038/ng875

Selcen, D. 2011. Myofibrillar myopathies. *Neuromuscul. Disord.* 21:161–171. http://dx.doi.org/10.1016/j.nmd.2010.12.007

Shah, S.B., F.C. Su, K. Jordan, D.J. Milner, J. Fridén, Y. Capetanaki, and R.L. Lieber. 2002. Evidence for increased myofibrillar mobility in desmin-null mouse skeletal muscle. *J. Exp. Biol.* 205:321–325.

Sjöberg, G., C.A. Saavedra-Matiz, D.R. Rosen, E.M. Wijsman, K. Borg, S.H. Horowitz, and T. Sejersen. 1999. A missense mutation in the desmin rod domain is associated with autosomal dominant distal myopathy, and exerts a dominant negative effect on filament formation. *Hum. Mol. Genet.* 8:2191–2198. http://dx.doi.org/10.1093/hmg/8.12.2191

Sjuve, R., A. Arner, Z. Li, B. Mies, D. Paulin, M. Schmittner, and J.V. Small. 1998. Mechanical alterations in smooth muscle from mice lacking desmin. *J. Muscle Res. Cell Motil.* 19:415–429. http://dx.doi.org/10.1023/A:1005353805699

Smythe, G.M., M.J. Davies, D. Paulin, and M.D. Grounds. 2001. Absence of desmin slightly prolongs myoblast proliferation and delays fusion in vivo in regenerating grafts of skeletal muscle. *Cell Tissue Res.* 304:287–294. http://dx.doi.org/10.1007/s004410100366

Thornell, L., L. Carlsson, Z. Li, M. Mericskay, and D. Paulin. 1997. Null mutation in the desmin gene gives rise to a cardiomyopathy. *J. Mol. Cell. Cardiol.* 29:2107–2124. http://dx.doi.org/10.1006/jmcc.1997.0446

Tidball, J.G. 1992. Desmin at myotendinous junctions. *Exp. Cell Res.* 199:206–212. http://dx.doi.org/10.1016/0014-4827(92)90425-8

Tokuyasu, K.T., A.H. Dutton, and S.J. Singer. 1983. Immunoelectron microscopic studies of desmin (skeletin) localization and intermediate filament organization in chicken skeletal muscle. *J. Cell Biol.* 96:1727–1735. http://dx.doi.org/10.1083/jcb.96.6.1727

van Spaendonck-Zwarts, K.Y., L. van Hessem, J.D.H. Jongbloed, H.E.K. de Walle, Y. Capetanaki, A.J. van der Kooi, I.M. van Langen, M.P. van den Berg, and J.P. van Tintelen. 2011. Desmin-related myopathy. *Clin. Genet.* 80:354–366. http://dx.doi.org/10.1111/j.1399-0004.2010.01512.x

Wang, X., H. Osinska, G.W. Dorn II, M. Nieman, J.N. Lorenz, A.M. Gerdes, S. Witt, T. Kimball, J. Gulick, and J. Robbins. 2001. Mouse model of desmin-related cardiomyopathy. *Circulation.* 103:2402–2407. http://dx.doi.org/10.1161/01.CIR.103.19.2402

Wieneke, S., R. Stehle, Z. Li, and H. Jockusch. 2000. Generation of tension by skinned fibers and intact skeletal muscles from desmin-deficient mice. *Biochem. Biophys. Res. Commun.* 278:419–425. http://dx.doi.org/10.1006/bbrc.2000.3810

Wilding, J.R., F. Joubert, C. de Araujo, D. Fortin, M. Novotova, V. Veksler, and R. Ventura-Clapier. 2006. Altered energy transfer from mitochondria to sarcoplasmic reticulum after cytoarchitectural perturbations in mice hearts. *J. Physiol.* 575:191–200. http://dx.doi.org/10.1113/jphysiol.2006.114116